0031-3998/03/5501-0093
PEDIATRIC RESEARCH
Vol. 55, No. 1, 2004
Printed in U.S.A.

The Effects of Systemic Magnesium Sulfate Infusion on Brain Magnesium Concentrations and Energy State During Hypoxia-Ischemia in Newborn Miniswine

JERRY B. GEE, II, RONALD J.T. CORBETT, JEFFREY PERLMAN, AND ABBOT R. LAPTOOK

Department of Pediatrics [J.B.G., J.P., A.R.L.], Department of Radiology [R.J.T.C.], University of Texas Southwestern Medical Center, Dallas, Texas, 75390-9063, U.S.A.

ABSTRACT

The mechanism of neuroprotection associated with systemically administered magnesium remains unclear. This investigation examined the acute effects of systemically administered $MgSO_4$ on brain extracellular ($[Mg]_{ecf}$) and intracellular ($[Mg]_i$) fluid Mg concentrations, specific brain phosphorylated metabolites, and brain intracellular pH. Miniswine were studied with P-31 magnetic resonance spectra, to derive $[Mg]_i$, and brain microdialysis probes, to measure $[Mg]_{ecf}$. Animals were infused with $MgSO_4$ ($n = 5$, 275 mg/kg over 30 min followed by 100 mg/kg over 30 min, designated MgHI) or Na_2SO_4 ($n = 5$, designated NaHI), and both groups underwent hypoxia-ischemia (HI) over the last 15 min of the infusions. Groups differed in plasma [Mg] at the completion of HI (9.1 ± 1.5 *versus* 1.1 ± 0.6 mM for MgHI and NaHI, respectively, $p < 0.05$). MgHI had elevations of $[Mg]_{ecf}$ (0.23 ± 0.11 and 0.40 ± 0.14 mM at control and completion of HI, respectively), and $[Mg]_{ecf}$ was unchanged for NaHI ($p < 0.05$ *versus* MgHI). At the completion of HI, MgHI had greater decreases in nucleoside triphosphate (NTP) (48 ± 6% of control), and more brain acidosis after HI (6.01 ± 0.07) compared with NaHI (NTP, 70 ± 3% of control; brain pH, 6.51 ± 0.14, both $p < 0.05$ *versus* MgHI). $[Mg]_i$ increased to elevated values during HI in both MgHI and NaHI ($p < 0.05$ *versus* control of each group) and remained higher in MgHI over the next 25 min ($p < 0.05$ *versus* NaHI). There were inverse correlations during HI between $[Mg]_i$ and brain NTP ($r^2 = 0.73$ and 0.59 for MgHI and NaHI, respectively), and brain acidosis ($r^2 = 0.85$ and 0.85 for MgHI and NaHI, respectively) in each group. These findings indicate complex effects of Mg on the brain. Elevation of $[Mg]_{ecf}$ may be beneficial with regards to excitatory neurotransmitters. However, greater disturbance of brain NTP concentration, more acidosis, and the increase in $[Mg]_i$ may offset any benefit. The results warrant further investigation using indicators of neuronal injury to determine whether Mg supplementation provides neuroprotection. **(*Pediatr Res* 55: 93–100, 2004)**

Abbreviations

HI, hypoxia-ischemia
HR, heart rate
MAP, mean arterial pressure
$[Mg]_{plasma}$, plasma Mg concentration
$[Mg]_{ecf}$, extracellular fluid Mg concentration
$[Mg]_i$, intracellular fluid Mg concentration
NTP, nucleoside triphosphate
^{31}P NMR, phosphorus 31 nuclear magnetic resonance
PCr, phosphocreatine
pHi, intracellular pH
Pi, inorganic phosphate

There has been keen interest in the use of magnesium as a potential neuroprotective intervention in perinatal medicine. Magnesium plays a critical role in the functioning of excitatory neurotransmitters, mostly at the postsynaptic level. It is a noncompetitive, voltage-dependent channel blocker acting on a modulatory site within the *N*-methyl-D-aspartate (NMDA) channel (1). This function is thought to allow magnesium to potentially block distal manifestations of the excitotoxic pathway. This is highly relevant inasmuch as excitatory neurotransmitters, such as glutamate, function as neurotoxins when in high concentrations in the brain extracellular fluid (ECF) (2). The latter occurs during hypoxia and/or ischemia due to excessive release of neurotransmitters as well as blockade of reuptake mechanisms (3). The high concentrations of excitatory transmitters stimulate surface receptors of neurons excessively and result in an influx of calcium, which in turn triggers a cascade of intracellular events culminating in tissue injury. There is specific interest in the neuroprotective effects of

Received December 31, 2002; accepted July 15, 2003.
Correspondence: Abbot R. Laptook, M.D., Department of Pediatrics, University of Texas Southwestern Medical Center, 5323 Harry Hines Blvd., Dallas, TX, 75390-9063, U.S.A.; e-mail: abbot.laptook@utsouthwestern.edu
Supported, in part, by a grant from the Wyeth Pediatrics Neonatology Research Fund.

DOI: 10.1203/01.PDR.0000099771.39629.E5

magnesium during the perinatal period. This is reflected by a broad experience with regard to the use of magnesium during pregnancy, including serum magnesium levels, knowledge of magnesium pharmacokinetics during pregnancy, the ready passage of magnesium across the placenta, and the tolerance of the fetus to elevated levels (4–8). The latter observations allow initiation of magnesium therapy before birth.

We have previously used newborn swine and brain microdialysis to demonstrate that increases in plasma concentration of magnesium result in entry into the brain ECF (9). Elevations in $[Mg]_{ecf}$, in turn, occur in an environment whereby interactions can readily occur at the neuronal cell surface. Although these observations support the prevalent focus of neuroprotection by magnesium, they also suggests the possibility that increases in $[Mg]_{ecf}$ could raise $[Mg]_i$. There has been very little work on alterations in $[Mg]_i$ in the perinatal period, but given magnesium's physiologic role as a calcium antagonist (10), there could be important intracellular effects of increases in $[Mg]_i$. Thus, the purpose of this study was to use brain microdialysis and P-31 magnetic resonance spectroscopy (MRS) to examine the effects of increases in plasma magnesium concentration on brain $[Mg]_{ecf}$, $[Mg]_i$, and brain phosphorylated metabolites and pHi before, during, and after HI in a newborn swine model.

METHODS

Experimental protocol. The study protocol was approved by the Institutional Animal Care and Research Advisory Committee of the University of Texas Southwestern Medical Center at Dallas. Animals were initially sedated with ketamine (20 mg/kg i.m.), followed by local skin infiltration of the neck with 1% Xylocaine, rapid tracheotomy, and initiation of mechanical ventilation using a 30:70 oxygen:nitrous oxide mixture. Analgesia was provided with nalbuphine (0.15 mg/kg i.m.) and muscle relaxation with tubocurarine Cl (0.1 mg/kg i.v.). Rectal temperature was maintained at 38–39°C using a heating pad. Catheters were placed in the external jugular vein and carotid artery. A 2-mm inflatable vascular occluder (In Vivo Metric, Healdsburg, CA, U.S.A.) was placed around the left common carotid artery and the tubing to control inflation/deflation was exteriorized. After local scalp infiltration with 1% Xylocaine and administration of sodium pentothal (20 mg/kg i.v.), the scalp was retracted, and a burr hole was made through which a loop-type microdialysis probe was inserted to a depth of 1 cm into the cerebral cortex and situated 1 cm anterior and lateral to the coronal and sagittal cranial sutures, respectively, for measurements of brain $[Mg]_{ecf}$. A 1 cm depth was used to insure that microdialysis samples were obtained from primarily gray matter of the cerebral cortex. A radiofrequency surface coil was then situated over the cranial vault for NMR data collection, and the animals were placed in a 4.7 T magnet. The microdialysis probes were positioned within the inner diameter of the surface coil (4 × 3 cm), on each side of the sagittal suture, with each probe 0.5–0.75 cm from the coil. Based upon prior work with phantoms, it is estimated that the majority of the NMR signal is derived from the first centimeter of cortex underneath the coil in the frontal, parietal, and occipital regions. Animals were allowed to stabilize for 3 1/2 hours before obtaining baseline values of HR, MAP, $[Mg]_{plasma}$, brain $[Mg]_{ecf}$, and brain intracellular energy metabolites over a 30-min period. Anesthesia was continued with 70% nitrous oxide along with intermittent doses of nalbuphine for analgesia.

Five miniswine (age 6 ± 3 d, wt 1.4 ± 0.4 kg, mean ± SD) were administered $MgSO_4$ and denoted MgHI. The target $[Mg]_{plasma}$ range was 4–6 mM based upon preliminary studies, which indicated that this was the highest concentration of Mg that could be tolerated without detrimental physiologic side-effects (9). Magnesium sulfate (30 mg of anhydrous powder per milliliter of H_2O; Sigma Chemical, St. Louis, MO, U.S.A.) was infused intravenously at a dose of 275 mg/kg body weight for 30 min, followed by 100 mg/kg for an additional 30 min in an effort to maintain $[Mg]_{plasma}$ at constant levels. Five miniswine (age 5 ± 3 d, wt 1.1 ± 0.3 kg) were administered Na_2SO_4 and denoted NaHI. Sodium sulfate (30 mg of anhydrous powder per milliliter of H_2O; Sigma Chemical) was administered in the NaHI group at a dose of 275 mg/kg followed by 100 mg/kg. HI was induced using the method of LeBlanc *et al.* (11). Ischemia was begun at 30 min of either $MgSO_4$ or Na_2SO_4 infusion by hemorrhagic hypotension to decrease MAP by one third, followed by induction of HI at 45 min of the infusions by inflating the vascular occluder and reducing the inspired oxygen to 10% for a 15-min interval. At the completion of the infusion, HI was terminated by changing the inspired gas concentration to 21%, deflating the vascular occluder, and reinfusing the withdrawn blood. The animals were studied an additional 4 h after the completion of HI. HR and MAP were monitored continuously and recordings were made every 30 min. Arterial pH and blood gases (partial pressures of O_2 and CO_2) were sampled every 30 min, and oxygen contents were determined at control, at the completion of HI, and at study completion. $[Mg]_{plasma}$ was measured every 15 min from the start of the infusion protocol for both groups. NMR measurements were obtained over successive 10-min intervals, and changes in $[Mg]_{ecf}$ were monitored by collecting consecutive 10-min samples using microdialysis as described below. At the end of the protocol, animals were killed using sodium pentobarbital (200 mg/kg, i.v.).

Microdialysis measurements. Loop-type microdialysis probes were constructed of commercially available hollow-fiber dialysis tubing (internal diameter = 150 μm, molecular weight cut-off = 17 kD; Spectrum Medical Industries Inc., Los Angeles, CA, U.S.A.) as described previously (9). After determination of the dead space from the probe to the effluent collection opening, probes were infused with artificial cerebrospinal fluid (154 mM NaCl, 1.3 mM $CaCl_2$, pH 7.2) at a rate of 5 μL/min and calibrated by dialysis against a standard solution with a known concentration of $MgSO_4$ (154 mM NaCl, 1.3 mM $CaCl_2$, and 1.0 mM $MgSO_4$). Recovery factors were determined from the ratio of total magnesium concentrations of the effluent and standard solutions, and were used to calculate the apparent $[Mg]_{ecf}$ from microdialysis fluid. Microdialysis data are presented at the midpoint of 10-min collection periods and corrected for real time by using the dead space determinations for each probe (*i.e.* 6–8 μL or 1.2–1.6 min). Through-

out the experiment, brain $[Mg]_{ecf}$ microdialysis samples of 50 μL volume were collected continuously every 10 min.

Magnesium concentration determinations. Total Mg was determined on 45 μL of microdialysis fluid and 10 μL of blood *via* atomic absorption spectroscopy at 285.2 nm (Spectra AA, Varian, Palo Alto, CA, U.S.A.) using an air/acetylene flame. Lanthanum oxide (0.5% wt/vol; Sigma Chemical) was added to reduce the potential for interferences from the incomplete dissociation of compounds in blood or microdialysis fluid, as recommended in the Varian analytical methods manual. Mg standard curves were prepared from stock $MgSO_4$ solutions.

NMR measurements. NMR measurements were made at 4.7 T using a double-tuned radiofrequency surface coil and protocol for interleaved ^1H and ^{31}P NMR data collection similar to that described previously (12). The collected ^1H NMR data were not used for this study. NMR data collection commenced 20 min before starting the $MgSO_4$ infusion and continued for 4 h after infusion. A 90° excitation pulse was applied at the ^{31}P frequency and its resulting free induction decay (FID) was acquired over 256 ms using a 5000-Hz sweep width and 2048 data points per FID; each spectrum was the sum of 200 FID (10 min per spectrum). The ^{31}P FID were processed by applying a baseline correction for DC offsets, left shifting to remove the first three data points, right shifting to re-establish phase integrity, apodization using an exponential filter corresponding to 10 Hz line broadening, zero filling once to 4096 data points, Fourier transformation, and baseline straightening *via* a spline interpolation routine. The chemical shift scale was calibrated with respect to PCr at 0.0 parts per million (ppm) in a control spectrum and the chemical shift locations of ^{31}P NMR peaks were determined by fitting individual peaks using a Lorentzian peak shape.

Data analysis. $[Mg]_i$ was calculated using the following formula (13):

$$[Mg]_i = K_D[(\sigma_{ATP} - \sigma_{\alpha-\beta})/(\sigma_{\alpha-\beta} - \sigma_{MgATP})] \quad (1)$$

where K_D is the apparent dissociation constant of MgATP, $\sigma_{\alpha-\beta}$ is the observed frequency difference between the α-ATP and β-ATP ^{31}P NMR peaks, and σ_{ATP} and σ_{MgATP} are the frequency differences between these two peaks in the absence and presence of saturating amounts of Mg, respectively. The K_D at a pH of 7.2, 37°C, and an ionic strength 0.15 used was 35 μM. K_D was adjusted specifically for the pHi, using the formula:

$$K_D^{pHi} = K_D^{7.2}[(1 + 10^{6.5-pHi})/(1 + 10^{6.5-7.2})] \quad (2)$$

The endpoints, σ_{ATP} and σ_{MgATP}, were adjusted for specific pH values using the formulas:

$$\sigma_{ATP} = -28.125 + 19.1812\,(pHi) - 3.0257\,(pHi)^2 + 0.15441\,(pHi)^3 \quad (3)$$

$$\sigma_{MgATP} = 16.6352 - 3.1071\,(pHi) + 0.38307\,(pHi)^2 - 0.01574\,(pHi)^3$$

Intracellular brain pH (pHi) was calculated from the chemical shift difference of inorganic phosphate (Pi) as described previously (14) using the following equation:

$$pH_{pi} = pK + \log[(p - \sigma_{HP})/(\sigma_p - p)] \quad (4)$$

where K is the apparent dissociation constant for Pi, σ_{HP} and σ_p equal the chemical shift at the acid and basic endpoints of the titration, respectively, and p equals the chemical shift difference in ppm between the Pi resonance frequency at different stages in the protocol and the PCr resonance at control (0 p.p.m.). Values of pK = 6.683, σ_{HP} = 3.153, and σ_p = 5.728 were selected for calculations of pH_{pi}, as described previously (14).

Changes in phosphorylated metabolites were examined by expressing the peak area of nucleoside triphosphate (NTP), Pi, and PCr during and after infusions of $MgSO_4$ or Na_2SO_4 as a percentage of values before infusions (control, set at 100%). NTP represents the average of the α, β, and γ NTP peaks. The average NTP concentration was used because preliminary analysis confirmed that the changes in the average of the γ, α, and β peaks are similar during ischemia to the change in the β-NTP alone. Use of the average reduces the variability associated with decreasing signal to noise of the NMR measurement during ischemia. The SD of phosphorylated metabolites during control was determined by expressing replicate values as a percentage of the first value and calculating the SD of the difference. All systemic data (HR, MAP, pH, blood gases, and hematocrit) as well as %PCr, %Pi, %NTP, pHi, $[Mg]_{plasma}$, $[Mg]_i$, and $[Mg]_{ecf}$ for each group were analyzed by two-way repeated measures ANOVA. Group interactions were further evaluated and localized by pair-wise comparisons (Student-Newman-Keuls). To facilitate and simplify the analysis, data collected in the postinfusion interval were grouped into 1-h blocks. Regression analysis was used to explore the relationship between $[Mg]_i$ and the cerebral energy state. A p value of < 0.05 was considered significant. All data are expressed as mean $\pm$ SD.

RESULTS

Arterial pH, blood gases, and oxygen contents were the same for both groups at control (Table 1). During HI, both groups demonstrated similar changes in pH but lower P_{O_2} values for the MgHI group. In spite of this, oxygen contents decreased to a similar extent in each group, indicating that MgHI and NaHI were comparable in the degree of induced hypoxia. There was a small decrease in P_{CO_2} in each group during HI, and this was different from control only for NaHI group. With the exception of a persistent acidosis, both groups demonstrated recovery to control values by 45 min after HI. MAP was similar between groups before HI (Fig. 1, *upper panel*). Both MgHI and NaHI had similar decreases in MAP during HI, and prompt increases in MAP to values similar to control shortly after resolution of HI. Patterns of changes in HR differed between MgHI and NaHI groups (Fig. 1, *lower panel*). NaHI animals had increases in HR above control values during HI, whereas MgHI animals had a decrease in HR leading to group differences at the end of HI.

Table 1. *Arterial pH, blood gases, and O_2 content during control, HI, and 45 min after HI*

Time	Group	pH	P_{O_2} (mm Hg)	P_{CO_2} (mm Hg)	O_2 Content (vol %)
Control	MgHI	7.41 ± 0.08	155 ± 35	38 ± 4	10.3 ± 1.7
	NaHI	7.42 ± 0.02	166 ± 16	35 ± 4	9.7 ± 0.5
End HI	MgHI	7.26 ± 0.14*	24 ± 3*	33 ± 5	2.3 ± 0.8*
	NaHI	7.20 ± 0.05*	30 ± 3*†	26 ± 5*	3.0 ± 0.6*
45 min postHI	MgHI	7.30 ± 0.12*	140 ± 29	39 ± 6	11.8 ± 2.4
	NaHI	7.33 ± 0.07*	168 ± 24	33 ± 3	12.2 ± 0.5*

* $p < 0.05$ *vs* control.
† $p < 0.05$ between groups.

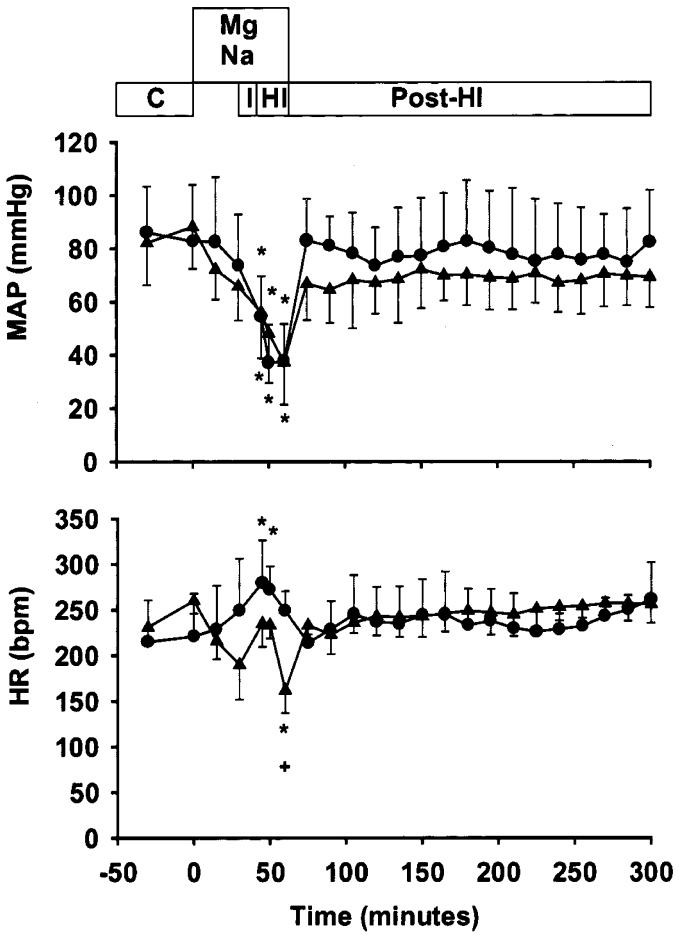

Figure 1. Changes in MAP (*upper panel*) and HR (*lower panel*) are plotted for MgHI (▲) and NaHI (●) groups. The times of control measurements (*C*), Na_2SO_4 and $MgSO_4$ infusions (*Na* and *Mg*, respectively), ischemia (*I*), hypoxia-ischemia (*HI*), and the period after HI (*Post-HI*) are indicated on the horizontal bars above the graphs. Values different from control are indicated by *asterisks* and differences between groups by *crosses* ($p < 0.05$).

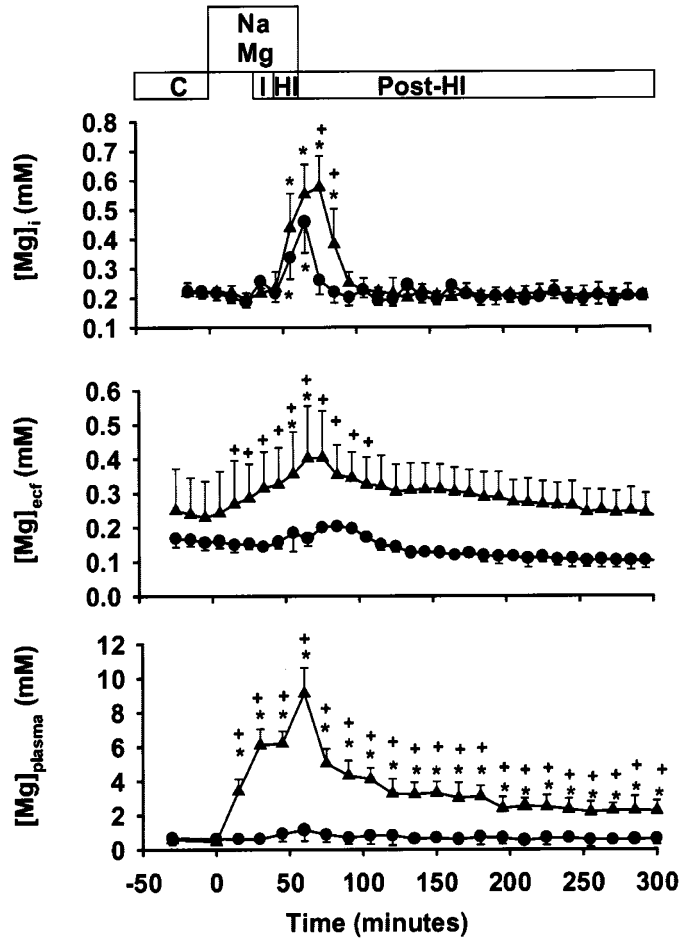

Figure 2. Magnesium concentrations of MgHI (▲) and NaHI (●) groups are plotted for fluid compartments of plasma ($[Mg]_{plasma}$, *lower panel*), brain extracellular fluid ($[Mg]_{ecf}$, *middle panel*) and brain intracellular fluid ($[Mg]_i$, *upper panel*). The times of control measurements (*C*), Na_2SO_4 and $MgSO_4$ infusions (*Na* and *Mg*, respectively), ischemia (*I*), hypoxia-ischemia (*HI*), and the period after HI (*Post-HI*) are indicated on the horizontal bars above the graphs. Values different from control are indicated by *asterisks* and differences between groups by *crosses* ($p < 0.05$).

Control values of $[Mg]_{plasma}$ were similar between groups, but differed both during and after HI (Fig. 2, *bottom panel*). During infusions of $MgSO_4$, $[Mg]_{plasma}$ was elevated above baseline, reached a peak value of 9.1 ± 1.5 mM at the end of HI, and decreased after completion of the infusion but remained significantly elevated throughout the remainder of the experiment. During the Na_2SO_4 infusion, $[Mg]_{plasma}$ rose slightly by the end of HI (0.65 ± 0.36 to 1.14 ± 0.64 mM), but was not statistically different. Values of $[Mg]_{ecf}$ at baseline were similar between groups (Fig. 2, *middle panel*). Infusion of $MgSO_4$ was associated with increases in $[Mg]_{ecf}$, which peaked at 74% above baseline values during HI (0.23 ± 0.11 to 0.40 ± 0.14mM). In contrast, infusion of Na_2SO_4 did not change $[Mg]_{ecf}$ during or after HI. Group differences for $[Mg]_{ecf}$ extended from 15 min of the respective infusions, through HI, and for 50 min after resolution of HI. Calculated $[Mg]_i$ values were similar between groups at control, and did not change with infusions of either $MgSO_4$ or Na_2SO_4 (Fig. 2, *top panel*). With the onset of HI, significant elevations of $[Mg]_i$ occurred

in both groups. At 15 and 25 min after HI, group differences were present, with higher values of $[Mg]_i$ in the MgHI group ($p < 0.05$).

Relative concentrations of phosphorylated metabolites (NTP, Pi, PCr) and brain pHi at control, during infusions of $MgSO_4$ or Na_2SO_4, and after hemorrhagic hypotension but before HI are listed in Table 2. Groups were similar in all variables until HI. The decreases in PCr and pHi at 45 min of the infusion reflects the effects of hemorrhagic hypotension initiated at 30 min of the infusion. During HI, infusion of $MgSO_4$ was associated with greater changes in NTP concentration compared with animals infused with Na_2SO_4. Specifically, the MgHI group had a maximal reduction in NTP to 48 ± 6% of control compared with a decrease to only 70 ± 3% in the NaHI group, and the maximum decrease occurred 5 min after HI. Differences between groups in NTP concentration extended from the last 5 min of HI until 25 min after HI (Fig. 3, *upper panel*). Accordingly, there was a greater change in Pi for the MgHI compared with NaHI groups (248 ± 49% *versus* 144 ± 20% of control at 5 min after HI, respectively, $p < 0.05$; data not shown). The larger changes in phosphorylated metabolites in the MgHI group were accompanied by greater brain acidosis. The pHi values for MgHI and NaHI groups were similar at control (6.99 ± 0.03 and 7.01 ± 0.02, respectively), but was lower at 15 min after HI in the MgHI group (6.01 ± 0.07) compared with the NaHI group (6.51 ± 0.14, $p < 0.05$). Group differences in pHi extended until 35 min after HI (Fig. 3, *bottom panel*). Values of PCr decreased to a similar extent for each group (14 ± 6% *versus* 13 ± 5% of control for MgHI and NaHI, respectively, at 5 min before completion of HI) and recovered to baseline levels by 25 min after HI (data not shown).

The relationship between $[Mg]_i$ and either brain NTP concentration or pHi during control and HI are plotted in Figure 4. For each group there was a strong and nearly identical inverse correlation between the reduction in NTP concentration relative to control and the increase in $[Mg]_i$ described by the following equations: $Y = -0.006X + 0.78$, $r^2 = 0.73$, $p < 0.001$ for MgHI, and $Y = -0.006X + 0.82$, $r^2 = 0.59$, $p < 0.001$ for NaHI (where $Y = [Mg]_i$ and $X =$ percentage NTP). Similarly, there was a strong and nearly identical inverse correlation between the extent of brain acidosis and the increase in $[Mg]_i$ described by the following equations: $Y = -0.32X + 2.44$, $r^2 = 0.85$, $p < 0.001$ for MgHI, and $Y = -0.29X + 2.23$, $r^2 = 0.85$, $p < 0.001$ for NaHI (where $Y = [Mg]_i$ and $X =$ pHi).

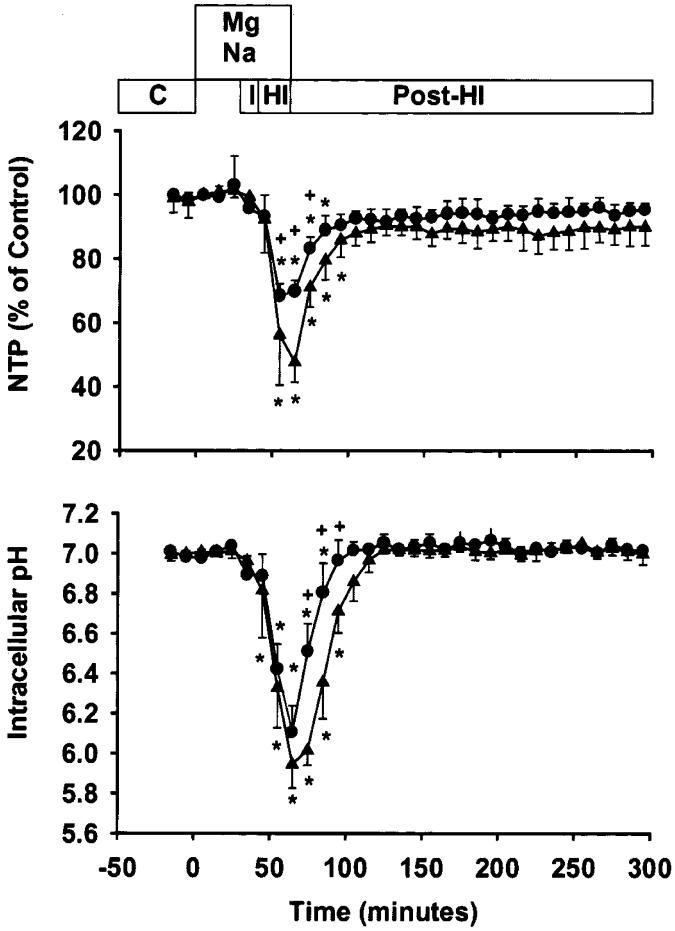

Figure 3. Changes in brain NTP (*upper panel*) and pHi (*lower panel*) are plotted for MgHI (▲) and NaHI (●) groups. Values for NTP are expressed as a percentage of control, with the latter set at 100%. The times of control measurements (*C*), Na_2SO_4 and $MgSO_4$ infusions (*Na* and *Mg*, respectively), ischemia (*I*), hypoxia-ischemia (*HI*), and the period after HI (*Post-HI*) are indicated on the horizontal bars above the graphs. Values different from control are indicated by *asterisks* and differences between groups by *crosses* ($p < 0.05$).

DISCUSSION

This investigation examined the effects of induced changes in plasma magnesium concentrations during and after HI on $[Mg]_{ecf}$, $[Mg]_i$, and on brain phosphorylated metabolites and pH using brain microdialysis and ^{31}P NMR in newborn swine. The principal findings of this investigation were 1) acute elevation in $[Mg]_{plasma}$ was readily associated with increases in

Table 2. *NMR measurements at control, after 25 min of infusions of either $MgSO_4$ or Na_2SO_4, and after 45 min of infusions before HI*

Time	Group	NTP*	Pi*	PCr*	pHi
Control	MgHI	98 ± 5	98 ± 9	98 ± 3	6.99 ± .03
	NaHI	98 ± 2	103 ± 6	101 ± 2	7.01 ± 0.2
Infusion + 25 min	MgHI	101 ± 2	100 ± 15	98 ± 3	7.01 ± .04
	NaHI	103 ± 9	102 ± 11	99 ± 4	7.04 ± .02
Infusion + 45 min**	MgHI	92 ± 10	115 ± 12	68 ± 24	6.81 ± .24
	NaHI	93 ± 7	121 ± 8	71 ± 13	6.89 ± .11

* Changes in phosphorylated metabolites (mean ± SD) represent the peak area during infusions as a percentage value of control (latter set at 100%). SD during control were based on replicate values as a percentage of the first value and calculating the SD of the difference.

** Values at 45 min of infusion represent the effects of hemorrhagic hypotension initiated at 30 min and before HI.

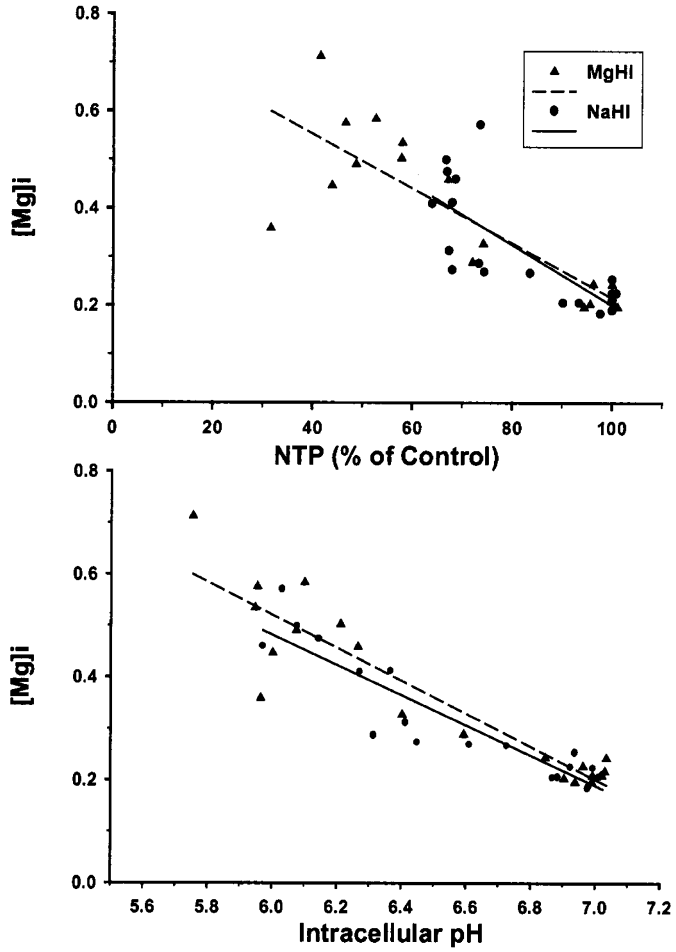

Figure 4. Scatter plots for intracellular Mg concentration ($[Mg]_i$) as a function of NTP concentration (*top panel*) and pHi (*lower panel*). Data are plotted for both the MgHI (▲) and NaHI (●) groups using values obtained at control, at 45 min of the protocol (during infusion of either $MgSO_4$ or Na_2SO_4, and the start of HI), at 55 min (during the infusions and 10 min of HI), and at 65 min (5 min after the termination of HI and completion of the infusions). These time points were chosen to capture the most prominent changes in brain energy state and acidosis. Regression lines for the MgHI and NaHI groups are represented by the *broken* and *solid lines*, respectively. Equations describing the regression lines are included in the text.

brain $[Mg]_{ecf}$; 2) increases in $[Mg]_i$ occur during HI in both $MgSO_4$ and Na_2SO_4 groups, but the increment was greater for animals with an acute elevation in $[Mg]_{plasma}$ and brain $[Mg]_{ecf}$; and 3) HI with hypermagnesemia was associated with greater alterations in NTP concentration and pHi than HI with a normal plasma [Mg]. Newborn miniswine were used because we have previously examined the relationship between systemic and brain magnesium concentrations in this model. Furthermore, newborn miniswine have been well characterized in this laboratory, including brain energy reserves and utilization rates (12), agonal glycolytic rate (15), and lactate/acid clearance (16). All of the latter processes reveal maturational changes over the first month and support newborn miniswine as a good model for neonatal events. However, newborn miniswine are probably more mature than newborn rodent models based upon energy utilization rates (12), magnitude of cerebral flow (CBF) (17), and ratio of PCr to NTP (12).

We have previously used newborn miniswine to demonstrate that acute increases in $[Mg]_{plasma}$ to 4–6 mM under normoxic/normotensive conditions results in an approximate doubling of brain $[Mg]_{ecf}$ (9). The present investigation adds to these observations by examining $[Mg]_{plasma}$ and brain $[Mg]_{ecf}$ during HI. Using the same dose and time of infusion of Mg as in our prior study (9), MgHI attained a plasma [Mg] of 6.4 ± 1.1 mM at 30 min of the infusion (before HI) that was similar to values in our prior report (5.7 ± 1.1 mM). Between 30 and 60 min of the infusion ($MgSO_4$ or Na_2SO_4) HI was associated with a further increase in $[Mg]_{plasma}$ to 9.1 ± 1.5 mM, higher than the value of 5.4 ± 1.1 mM achieved under normoxic/normotensive conditions. The reason for the higher $[Mg]_{plasma}$ during HI is unclear but may reflect redistribution of cardiac output and an altered volume of distribution (not measured). In spite of differences in $[Mg]_{plasma}$ during normoxia and HI, the increase in $[Mg]_{ecf}$ was similar. This suggests a limitation of Mg entry into the brain during HI relative to normoxia. This could be secondary to decreased brain Mg delivery and would be consistent with the pronounced ischemic changes noted in brain energy state even though plasma levels were raised. Saturation of transport mechanisms for Mg entry into the brain is another possibility.

Systemic physiologic variables before and during HI were well matched among the groups in spite of different plasma [Mg]. An important difference between groups was the pattern of HR change with reductions in HR during HI in Mg-infused animals and increases in HR in Na_2SO_4 infused. Reduction in HR with Mg supplementation has been reported previously in newborn swine under normoxic conditions from this laboratory (9) and others (18). The reduction in HR is part of global hemodynamic changes associated with hypermagnesemia, the most consistent of which is a dose-related reduction in systemic vascular resistance (19, 20). The blood pressure response in turn depends on the cardiac output, which will reflect a dose-dependent negative inotropic effect of Mg. These effects may contribute to the observation that MgHI animals had greater reductions in NTP and brain acidosis compared with NaHI. This occurred in the presence of similar changes in MAP and systemic oxygenation (indicated by O_2 content). Given the vasodilatory effect of Mg on cerebral vessels (21), different cerebral flow (CBF) during and after HI among the two groups is a potential etiology for the changes in NTP and pHi. Reduction in CBF during HI would be expected to be associated with progressive vasodilation. Additional vasodilatory stimuli such as hypermagnesemia may promote greater reductions in CBF at the same blood pressure compared with animals with a normal [Mg].

Calculated values of $[Mg]_i$ before infusions and HI were identical in each group (0.22 mM), and were lower than other values for brain using either ion-selective electrodes [0.46 mM (22)], or Mg indicators such as Mag-Fura-2-acetoxymethyl ester [0.48 mM (23)]. In part, this may reflect the specific algorithm used to derive $[Mg]_i$ using P31-MRS data, as previously demonstrated in this laboratory (13). Irrespective of the absolute value of $[Mg]_i$, both groups had significant increases in $[Mg]_i$ during or immediately after HI that was higher in the

$MgSO_4$ group (164% above control) compared with the Na_2SO_4 group (109% above control).

Based upon the results of this study, the most likely reason for the observed increase in $[Mg]_i$ and differences between groups in $[Mg]_i$ are the changes in brain phosphorylated metabolites and pHi. Thus, the metabolic pattern of increased $[Mg]_i$, brain acidosis, reduced NTP and PCr, and increased inorganic phosphorus is consistent with utilization of NTP and release of intracellular bound magnesium. This pattern of change has been noted in adults with stroke (24) and in guinea pig brain *in vitro* during severe hypoxia and hypoglycemia (25). The strong, inverse correlations between $[Mg]_i$ and both the reduction in NTP concentration and the extent of brain acidosis for both groups are supportive of this concept (Fig. 4). Furthermore, the greater change in $[Mg]_i$ for the MgHI compared with the NaHI group most likely reflects greater alterations in the brain energy state during HI.

There are other possibilities for the observed increase in $[Mg]_i$ during HI. First, magnesium could be transported from the ECF into cells. Although regulation of $[Mg]_i$ is not completely understood (26), there are data to support a reversible, ATP-independent, Na^+-Mg^{+2} antiport in isolated leech neurons (22). In the latter, increasing the $[Mg]_{ecf}$ increased $[Mg]_i$ and decreased both $[Na]_i$ and membrane depolarization; a reduction in $[Mg]_{ecf}$ had the opposite effect. In contrast to magnesium efflux, use of amiloride to inhibit the Na^+-Mg^{+2} antiport suggested that most of the magnesium influx occurs through passive pathways and not reversal of the Na^+-Mg^{+2} antiport (22). Transport/influx of magnesium could be secondary to the elevated $[Mg]_{ecf}$ in MgHI animals, however, this is not consistent with the unchanged $[Mg]_{ecf}$ in the NaHI group. A second possibility is neuron depolarization. In cultured dorsal root ganglion neurons of newborn rats, depolarization is associated with a 3-fold increase in $[Mg]_i$ (23, 27). The increase in $[Mg]_i$ occurred in the absence of $[Mg]_{ecf}$, and the increase disappeared in the absence of extracellular calcium. These observations suggest that depolarization causes an influx of calcium, which in turn releases Mg from intracellular organelles such as mitochondria, and endoplasmic reticulum (27). A final possibility for the increase in $[Mg]_i$ is chemical stimulation. Vasopressin (28), bradykinin (29), and cholecystokinin (30) can increase $[Mg]_i$ in vascular and nonvascular tissue outside of the CNS. Glutamate can induce increases in $[Mg]_i$ in cultured rat cortical neurons (31). In contrast to depolarization, the mechanism for glutamate-stimulated increases in $[Mg]_i$ involves Mg entry through NMDA-activated ion channels (32). Based on prior study of HI in neonatal animal models (3, 33), it is expected that brain glutamate would be increased for both MgHI and NaHI groups.

The clinical implications of an increased brain $[Mg]_i$ during and immediately after HI are unclear. Raising the $[Mg]_i$ may contribute to the putative neuroprotection mechanisms associated with magnesium. For example, magnesium is a physiologic antagonist to calcium (10). It has been speculated that the calcium-mediated rise in $[Mg]_i$ with neuronal depolarization may serve as an important negative feedback to suppress neuronal excitation (27). Furthermore, an increase in $[Mg]_i$ after depolarization may be critical for maintaining regulation of ionic channels in the face of elevated intracellular calcium (27). Increased intracellular calcium associated with HI is a critical focal point of the excitotoxic pathway to brain injury, and increases in $[Mg]_i$ may counter these effects in a parallel fashion to depolarization. However, if the increased $[Mg]_i$ merely reflects the extent of brain energy failure, then neuroprotection provided by increases of $[Mg]_i$ is doubtful. Furthermore, if physiologic effects mediated by $[Mg]_i$ (*e.g.* enzyme activation, ionic channel regulation, maintenance of protein conformation) are dependent on a constant $[Mg]_i$, then benefit may not be expected from Mg supplementation therapy. Interestingly, there are a number of studies that report a reduced $[Mg]_i$ associated with head trauma, and that Mg supplementation obviated the decrease in $[Mg]_i$ and attenuated the extent of neurologic injury (34, 35).

The results of this investigation demonstrate that Mg supplementation has extremely complex effects on the brain. Ultimately, the only way to ascertain whether Mg supplementation provides neuroprotection is to perform parallel experiments with markers of brain injury as outcome variables, including both histologic and neurobehavioral assessments. In view of the complexity of performing brain microdialysis to measure $[Mg]_{ecf}$ and simultaneous brain biochemical assessments using ^{31}P NMR during and after HI, this investigation focused on immediate perturbations of these variables. Given these limitations, the results of this investigation suggest that the presence or absence of neuroprotection associated with Mg supplementation will probably reflect a net function of Mg effects in the brain ECF, intracellular compartment, and on the determinants of brain phosphorylated metabolites and pH. Increasing $[Mg]_{ecf}$ is expected to be beneficial because there is blockade of NMDA receptor activity and limitation of calcium influx, in addition to possible inhibition of lipid peroxidation (36). In contrast, for the reasons discussed above, increasing $[Mg]_i$ may have beneficial or detrimental effects on the brain. The effect of Mg on the brain energy state during acute HI is expected to be detrimental. Greater energy failure with HI (primary energy failure) is correlated with subsequent secondary energy failure, and ultimately histologic evidence of brain injury (37).

These divergent biochemical and physiologic effects of Mg therapy may provide insights into the discrepant reports regarding magnesium as a potential neuroprotective therapy in both animals (38–45) and humans (46–48). Magnesium administration either before or after HI, ischemia, or excitotoxic exposure in perinatal and adult rats ameliorated the extent of neurologic injury (38–43). In contrast, systemic magnesium administration after HI in newborn piglets did not prevent the development of delayed energy failure, but much lower $[Mg]_{plasma}$ were achieved compared with the present study (44). Furthermore, systemic magnesium administration after asphyxia in fetal sheep did not reduce the extent of cytotoxic edema, did not improve the recovery of the EEG, and did not alter the histologic outcome (45). Retrospective epidemiologic human data, however, suggests that *in utero* exposure of the fetus to magnesium is associated with less cerebral palsy in children of very low birth weight (46, 47). The latter observations have been questioned because $MgSO_4$ has not been found

to reduce the incidence of cranial ultrasound abnormalities that are strong predictors of cerebral palsy in preterm infants (48). Uncertainties over the neuroprotective role of magnesium therapy could be clarified by further study of magnesium supplementation on brain damage assessed several days after HI using the newborn swine model presented here.

Acknowledgments. The authors thank William Gitomer, Ph.D., and the staff of the Mineral and Metabolism Laboratory at Parkland Hospital, Dallas, TX.

REFERENCES

1. Nowak L, Bregestovski P, Ascher P, Herbet A, Prochiantz A 1984 Magnesium gates glutamate-activated channels in mouse central neurons. Nature 307:462–465
2. Lipton SA, Rosenberg PA 1994 Excitatory amino acids as a final common pathway for neurologic disorders. N Engl J Med 330:613–622
3. Hagberg H, Lehmann A, Sandberg M, Nystrom B, Jacobson I, Hamberger A 1985 Ischemia-induced shift of inhibitory and excitatory amino acids from intra- to extracellular compartments. J Cereb Blood Flow Metab 5:413–419
4. Rasch DK, Huber P, Richardson CJ, L'Hommedieu CS, Nelson TE, Reddi R 1982 Neurobehavioral effects of neonatal hypermagnesemia. J Pediatr 100:272–276
5. Stone SR, Pritchard JA 1970 Effect of maternally administered magnesium sulfate on the neonate. Obstet Gynecol 35:574–577
6. Green KW, Key TC, Coen R, Resnik R 1983 The effects of maternally administered magnesium sulfate on the neonate. Am J Obstet Gynecol 146:29–33
7. Cunningham FG, MacDonald PC, Grant NF 1989 Hypertensive disorders in pregnancy. In: Cunningham FG, MacDonald PC, Gant NF (eds) Williams Obstetrics, 18th Ed. Appleton and Lange, Norwalk, CT, pp 653–694
8. Hallak M, Cotton DB 1993 Transfer of maternally administered magnesium sulfate into the fetal compartment of the rat: assessment of amniotic fluid, blood, and brain concentrations. J Obstet Gynecol 169:427–431
9. Gee JB, Corbett RJT, Perlman JM, Garcia D, Laptook AR 1999 Age-dependent differences in the relationship between plasma and brain extracellular fluid concentrations of magnesium after $MgSO_4$ infusions in miniswine. Pediatr Res 46:281–286
10. Iseri LT, French JH 1984 Magnesium: nature's physiologic calcium blocker. Am Heart J 108:188–193
11. LeBlanc MH, Farias LA, Markov AK, Evans OB, Smith B, Smith EE, Brown EG 1991 Fructose-1,6-diphosphate, when given five minutes after injury, does not ameliorate hypoxic ischemic injury to the central nervous system in the newborn pig. Biol Neonate 59:98–108
12. Corbett RJT, Laptook AR, Garcia D, Ruley JI 1993 Energy reserves and utilization rates in developing brain measured *in vivo* by ^{31}P and ^{1}H nuclear magnetic resonance spectroscopy. J Cereb Blood Flow Metab 13:235–246
13. Corbett RJT, Gee J, Laptook AR 1996 Calculation of intracellular cerebral [Mg^{2+}] during hypoxic ischemia by *in vivo* ^{31}P NMR. Neuroreport 8:287–291
14. Corbett RJT, Laptook AR, Nunnally RL 1987 The use of the chemical shift of the phosphomonoester P-31 magnetic resonance peak for the determination of intracellular pH in the brains of neonates. Neurology 37:1771–1779
15. Corbett RJT, Laptook AR, Ruley JI, Garcia D 1991 The effect of age on glucose modulated cerebral agonal glycolytic rates measured *in-vivo* by 1H NMR spectroscopy. Pediatr Res 30:579–586
16. Corbett R, Laptook A, Kim B, Tollefsbol G, Silmon S, Garcia D 1999 Maturational changes in cerebral lactate and acid clearance following ischemia measured *in vivo* using magnetic resonance spectroscopy and microdialysis. Brain Res Dev Brain Res 113:37–46
17. Laptook AR, Peterson J, Porter AM 1987 Cerebral lactic acid delivery and uptake during and after ischemia in the piglet. Neurology 37:1549–1552
18. Rivera LI, Gootman PM, Brust M, Condemi G, Hundley BH, Lin RH, Cohen HL, Gandhi MR, Altura BT, Gootman N 1990 Unusual observations on hypermagnesemic levels and cardiorespiratory effects in neonatal swine. Magnes Trace Elem 9:124–131
19. Caspi J, Coles JG, Benson LN, Herman SL, Augustine J, Wilson GJ 1994 Dose related effects of magnesium on myocardial function in the neonate. Hypertension 23:174–178
20. James MFM, Cork RC, Dennett JE 1987 Cardiovascular effects of magnesium sulphate in the baboon. Magnesium 6:314–324
21. Kim C-R, Oh W, Stonestreet BS 1997 Magnesium is a cerebrovasodilator in newborn piglets. Am J Physiol 272:H511–H516
22. Günzel D, Schlue W-R 1996 Sodium-magnesium antiport in Retzius neurones of the leech *Hirudo medicinalis*. J Physiol 491:595–608
23. Kato H, Gotoh H, Kajikawa M, Suto K 1998 Depolarization triggers intracellular magnesium surge in cultured dorsal root ganglion neurons. Brain Res 779:329–333
24. Helpern JA, Vande Linde AM, Welch KM, Levine SR, Schultz LR, Ordidge RJ, Halvorson HR, Hugg JW 1993 Acute elevation and recovery of intracellular [Mg^{2+}] following human focal cerebral ischemia. Neurology 43:1577–1581
25. Brooks KJ, Bachelard HS 1989 Changes in intracellular free magnesium during hypoglycaemia and hypoxia in cerebral tissue as calculated from ^{31}P-nuclear magnetic resonance spectra. J Neurochem 53:331–334
26. Romani A, Scarpa A 1992 Regulation of cell magnesium. Arch Biochem Biophys 298:1–12
27. Gotoh H, Kajikawa M, Kato H, Suto K 1999 Intracellular Mg^{2+} surge follows Ca^{2+} increase during depolarization in cultured neurons. Brain Res 828:163–168
28. Touyz RM, Schiffrin EL 1996 Angiotensin II and vasopressin modulate intracellular free magnesium in vascular smooth muscle cells through Na^{+}-dependent protein kinase C pathways. J Biol Chem 271:24353–24358
29. Sebille S, Millot JM, Maizieres M, Arnaud M, Delabroise AM, Jacquot J, Manfait M 1996 Spatial and temporal Mg^{2+} signaling in single human tracheal gland cells. Biochem Biophys Res Commun 227:743–749
30. Gaeda M, Singh J, Domschke W, Mooren F Ch, Wisdom DM 1996 Secretagogue-evoked mobilization of magnesium in mouse pancreatic acini. J Physiol 493:90–91
31. Brocarad JB, Rajdev S, Reynolds IJ 1993 Glutamate-induced increases in intracellular free Mg^{2+} in cultured cortical neurons. Neuron 11:751–757
32. Stout AK, Li-Smerin Y, Johnson JW, Reynolds IJ 1995 Mechanisms of glutamate-stimulated Mg^{2+} influx and subsequent Mg^{2+} efflux in rat forebrain neurons in culture. J Physiol 492:3:641–657
33. Andiné P, Sandberg M, Bågenholm R, Lehmann A, Hagberg H 1991 Intra- and extracellular changes of amino acids in the cerebral cortex of the neonatal rat during hypoxic-ischemia. Dev Brain Res 64:115–120
34. Vink R, McIntosh TK, Demediuk P, Weiner M, Faden AI 1988 Decline in intracellular free Mg^{2+} is associated with irreversible tissue injury after brain trauma. J Biol Chem 263:757–761
35. Bareyre FM, Saatman KE, Helfaer MA, Sinson G, Weisser JD, Brown AL, McIntosh TK 1999 Alterations in ionized and total blood magnesium after experimental traumatic brain injury: relationship to neurobehavioral outcome and neuroprotective efficacy of magnesium chloride. J Neurochem 73:271–280
36. Regan RF, Jasper E, Guo Y, Panter SS 1998 The effect of magnesium on oxidative neuronal injury *in vitro*. J Neurochem 70:77–85
37. Blumberg RM, Cady BE, Wigglesworth JS, McKenzie JE, Edwards AD 1997 Relation between delayed impairment of cerebral energy metabolism and infarction following transient focal hypoxia-ischaemia in the developing brain. Exp Brain Res 113:130–137
38. McDonald JW, Silverstein FS, Johnston MV 1990 Magnesium reduces *N*-methyl-D-aspartate (NMDA)-mediated brain injury in perinatal rats. Neurosci Lett 109:234–238
39. Wolf G, Keilhoff G, Fischer S, Hass P 1990 Subcutaneously applied magnesium protects reliably against quinolinate-induced *N*-methyl-D-aspartate (NMDA)-mediated neurodegeneration and convulsions in rats: are there therapeutical implications? Neurosci Lett 117:207–211
40. McIntosh TK, Vink R, Yamakami I, Faden AI 1989 Magnesium protects against neurological deficit after brain injury. Brain Res 482:252–260
41. Izumi Y, Roussel S, Pinard E, Seylaz J 1991 Reduction of infarct volume by magnesium after middle cerebral artery occlusion in rats. J Cereb Blood Flow Metab 11:1025–1030
42. Thordstein M, Bågenholm R, Thiringer K, Kjellmer I 1993 Scavengers of free oxygen radicals in combination with magnesium ameliorate perinatal hypoxic-ischemic brain damage in the rat. Pediatr Res 34:23–26
43. Tsuda T, Kogure K, Nishioka K, Watanabe T 1991 Mg^{2+} administered up to twenty-four hours following reperfusion prevents ischemic damage of the CA1 neurons in the rat hippocampus. Neuroscience 44:335–341
44. Penrice J, Amess PN, Punwani S, Wylezinska M, Tyszczuk L, D'Souza P, Edwards AD, Cady EB, Wyatt JS, Reynolds EO 1997 Magnesium sulfate after transient hypoxia-ischemia fails to prevent delayed cerebral energy failure in the newborn piglet. Pediatr Res 41:443–447
45. de Haan HH, Gunn AJ, Williams CE, Heymann MA, Gluckman PD 1997 Magnesium sulfate therapy during asphyxia in near-term fetal lambs does not compromise the fetus but does not reduce cerebral injury. Am J Obstet Gynecol 176:18–27
46. Nelson KB, Grether JK 1995 Can magnesium sulfate reduce the risk of cerebral palsy in very low birthweight infants? Pediatrics 95:263–269
47. Schendel DE, Berg CJ, Yeargin-Allsop M, Boyle CA, Decoufle P 1996 Prenatal magnesium sulfate exposure and the risk for cerebral palsy or mental retardation among very low-birth-weight children aged 3 to 5 years. JAMA 276:1805–1810
48. Leviton A, Paneth N, Susser M, Reuss ML, Allred EN, Kuban K, Sanocka U, Hegyi T, Hiatt M, Shahrivar F, Van Marter LJ 1997 Maternal receipt of magnesium sulfate does not seem to reduce the risk of neonatal white matter damage. Pediatrics 99:E2